

Supplementary Information

Unleashing the High Energy Potential of Zinc-Iodide Batteries: High-Loaded Thick Electrodes Designed with Zinc Iodide as the Cathode

Jingkang Ma^{a,b}, Alireza Azizi^c, Erhuan Zhang^d, Hong Zhang^{b,*}, Anqiang Pan^{c,e,*}, and Ke Lu^{a,*}

^aInstitutes of Physical Science and Information Technology, Key Laboratory of Structure and Functional Regulation of Hybrid Materials of Ministry of Education, Anhui University, Hefei, Anhui 230601, China.

*Email: luke@ahu.edu.cn (K.L.)

^bSchool of Chemistry and Chemical Engineering, Harbin Institute of Technology, Harbin, Heilongjiang 150001, China. *Email: zhanghonghit@hit.edu.cn (H.Z.)

^cSchool of Materials Science and Engineering, Central South University, Hunan, Changsha 410083, China.

*Email: pananqiang@csu.edu.cn (A.P.)

^dGlobal Institute of Future Technology, Shanghai Jiao Tong University, Shanghai 200240, China.

^eSchool of Physics and Technology, Xinjiang University, Urumqi, Xinjiang, 830046, China.

Experimental details

Materials synthesis

Preparation of ZIF-8¹: In a typical synthetic process, 30 g $\text{Zn}(\text{CH}_3\text{COO})_2 \cdot 2\text{H}_2\text{O}$ was dissolved in 500 ml of deionized water under magnetic stirring (Denoted as solution A). 91 mg cetyltrimethylammonium bromide (CTAB) and 112 g 2-methylimidazole were dissolved in 500 mL of deionized water stirred to form a homogeneous solution (Denoted as solution B). Then, the solution A was added into solution B under magnetic stirring for 20 min and aged for 4 h at room temperature. After aging, the product was collected by centrifuging, washing several times with deionized water and drying at 60°C for 12 h to obtain the ZIF-8.

Preparation of N-Doped Porous Carbon: The ZIF-8 precursors were heated at a temperature of 950 °C for 3h in a tube furnace under N_2 flow to obtain the N-doped carbon, which were labeled as NC.

Preparation of NC-Co: Typically, 100 mg NC powder was dispersed in 100 mL 0.1M $\text{Co}(\text{NO}_3)_2$ solution to prepare the NC-Co²⁺ sample. Then sample was collected by centrifugation and then dried at 60°C in a vacuum oven for 5 hours. After that, thermal activation was performed at 800°C for 2 hours in nitrogen/hydrogen to generate the final products (NC-Co).

Preparation of NC-Co/ ZnI_2 ²: Zinc iodide was adsorbed onto the porous support by the "solution-adsorption" method. First, 300 mg of zinc iodide was placed in ethanol to obtain a supersaturated solution of zinc iodide. 53 mg of NC-Co was added into this solution and stirred for 30 min. Then, the prepared composites were dried at 60 °C for 12 h to remove the ethanol. After drying, the final product was obtained and denoted as NC-Co/ ZnI_2 .

Sample characterization:

Scanning electron microscopy (SEM) images and Transmission electron microscopy (TEM) were acquired using Hitachi 650 electron microscope and JEM-2100F microscope with a Bruker EDS detector, respectively. N_2 adsorption-desorption isotherms were recorded on a TriStar 3000 analyzer and 3Flex 3500 at 77 K. X-ray diffraction patterns were performed using a Rigaku Miniflex diffractometer (Rigaku Corporation, Japan). Specifically, the ZnI_2/I_2 -loaded porous materials were dried at 80 °C for 10 h to remove the surface adsorbed iodine and water. Nitrogen adsorption-desorption isotherms were measured with a Kubo X1000 instrument at 77 K. Before measurement, the samples were degassed at 95 °C for 6 h on a vacuum line. The specific surface areas were calculated by the Brunauer-Emmett-Teller (BET) method. Pore size distribution curves were computed from the desorption branches of the isotherms using the Barrett, Joyner, and Halenda (BJH) method. X-ray diffraction patterns were performed using a Rigaku Miniflex diffractometer (Rigaku Corporation, Japan). X-ray photoelectron spectroscopy (XPS) measurements were carried out on an ESCALAB 250 X-ray photoelectron spectrometer. The specific surface areas and pore size distributions were calculated by the Brunauer-Emmett-Teller (BET) and Barret-Joyner-Halenda (BJH) methods. The Raman spectra were collected using LabRAM HR 800 system with a 532 nm excitation laser. UV-Vis analysis was measured using a Shimadzu UV-1800 spectrophotometer.

Electrochemical measurements: Typically, the ZnI_2 /matrix composite were mixed with Carbon black and polyvinylidene fluoride (PVDF) with a weight ratio of 8.5:1:0.5. Then, the mixture was dispersed in a small methyl-2-pyrrolidinone (NMP) solvent by grinding in an agate mortar to obtain a homogeneous slurry. Then the slurry was coated onto Al foil current collector followed by drying under vacuum at 60 °C for 12 h. For the coin cell, the CR2025 coin-type cell was assembled with iodine cathode, Zn plate anode and glass fiber separator in 2 M ZnSO_4 electrolyte. The pouch cell was assembled in aluminum-plastic film with the above iodine cathode, Zn foil anode and glass fiber separator using 2 M ZnSO_4 as electrolyte. The Cyclic voltammetric (CV) curves are carried out using CHI 660e/DH7000 electrochemical workstation. Electrochemical impedance spectra were collected using a Gamry Reference 600 potentiostat in the frequency range of 100 kHz to 100 mHz and an AC amplitude of 5 mV. The galvanostatic charge/discharge were tested between 0.4-1.6V on a Neware battery tester. All the electrochemical experiments were performed at room temperature. The specific capacity was normalized to the mass of cathode.

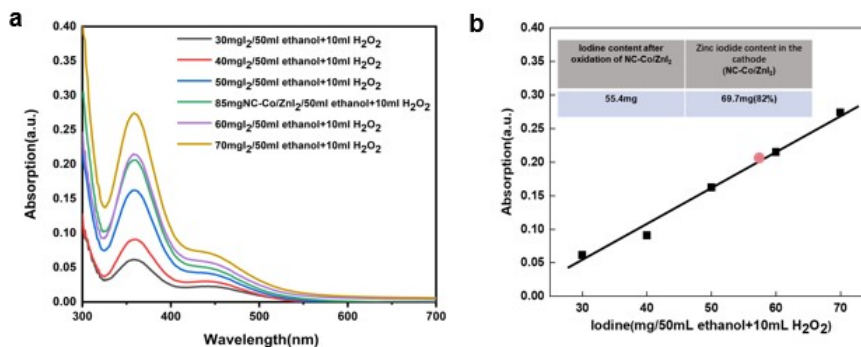


Figure. S1 (a) The typical absorption spectra of iodine with different concentrations and 85mg NC-Co/ZnI₂ dissolved in ethanol and H₂O₂. The linear relationship between the UV absorbance and the concentrations of iodine. (b) The linear relationship between the UV absorbance and the concentrations of iodine. The inset shows the calculated mass of iodine after oxidation by NC-Co/ZnI₂ as well as the initial zinc iodide loading.

As shown in Figure S1a in ethanol solution, the optical absorption spectra exhibit a characteristic absorption peak of I₂ at 360 nm in ethanol /H₂O₂ solution. The absorbance at 360 nm was recorded for each sample and plotted against the iodine content of the solution. (Figure S1b). According to the Lambert-Beer law ($A = \epsilon \times b \times c$), a linear relationship between the concentration of iodine (c) and the absorbance of the typical peak (A) was obtained, which was used to determine the content of iodine in solution.³ The amount of ZnI₂ was calculated by the equation: $2\text{ZnI}_2 + \text{H}_2\text{O}_2 \rightarrow 2\text{Zn}(\text{OH})_2 + 2\text{I}_2$.

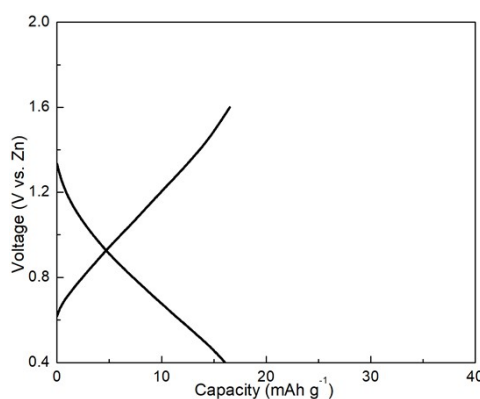


Figure S2. Galvanostatic charge-discharge profile of Co/NC without iodine loading.

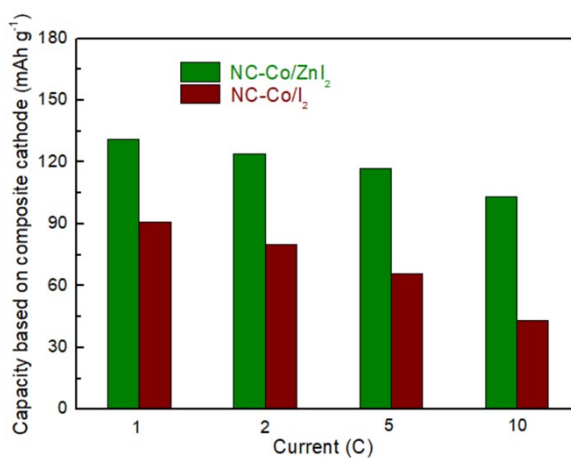


Figure S3. Comparison of different samples in terms of rate capability. The specific capacity was normalized to the mass of cathode.

Table S1. Comparison of cell performance with other recently reported aqueous of Zn-I₂ battery.

Cathodes	Active component content (%)	Discharge capacity (mAh g _{cathode} ⁻¹)	Capacity retention/cycles/current density
NC-Co/ZnI ₂	82	130	85.4%/10000/1C
NHPC/I ₂ ⁴	61.6	110.8	58.3%/10000 /5.0 C
MPC/I ₂ ⁵	41	46.6	60%/2,000 /5.0 C
GC-PAN/I ₂ ⁶	32	37.4	97.24%/2000/20C
OSTC/I ₂ ⁷	45.8	67	85.4%/10000/1 A g ⁻¹
LiVS ₂ /I ₂ ⁸	60.7	94.3	86%/30000/5 A g ⁻¹
CMK-3/I ₂ ⁹	60	37.8	80.6/39000/10 A g ⁻¹
B-Fe-NC/I ₂ ¹⁰	30	37	99.7%/5000/1C
PNC-1000/I ₂ ¹¹	58	81.2	89%/10000/1 A g ⁻¹
NCCs/I ₂ ¹²	50	103.6	100%/1000/0.1 A g ⁻¹

Table S2. Comparison of the electrochemical performance of Zn-I₂ pouch cells assembled with different parameters.

Zn-I ₂ pouch cell	N/P ratio	Capacity	Capacity retention	Energy density (Wh kg _{cathode+anode} ⁻¹)	N/P ratio:	E/S ratio	Capacity	Capacity retention	Energy density (Wh kg _{cathode+anode+electrolyte} ⁻¹)
		1.2	45%/50 cycle	66			2.5	35%/50 cycle	26
		2.1	85%/50 cycle	48	2.1		3.4	85%/50 cycle	22
		6.8	87%/50 cycle	19			7.9	86%/50 cycle	13
		18.5	88%/50 cycle	7.5			12.2	89%/50 cycle	9.1

Reference

- Jiang, Y.; Yu, Z. X.; Zhou, X. F.; Cheng, X. L.; Huang, H. J.; Liu, F. F.; Yang, Y. X.; He, S. N.; Pan, H. G.; Yang, H.; Yao, Y.; Rui, X. H.; Yu, Y., Single-Atom Vanadium Catalyst Boosting Reaction Kinetics of Polysulfides in Na-S Batteries. *Adv. Mater.* **2023**, *35* (8), 2208873.
- Zhang, H.; Shang, Z. T.; Gao, S. Y.; Song, B.; Zhang, W. L.; Cao, R. G.; Jiao, S. H.; Cheng, Y. W.; Chen, Q. W.; Lu, K., Redox catalysis-promoted fast iodine kinetics for polyiodide-free Na-I₂ electrochemistry. *J. Mater. Chem. A* **2022**, *10* (21), 11325-11331.

3. Lu, K.; Hu, Z. Y.; Ma, J. Z.; Ma, H. Y.; Dai, L. M.; Zhang, J. T., A rechargeable iodine-carbon battery that exploits ion intercalation and iodine redox chemistry. *Nat. Commun.* **2017**, *8*, 527.
4. Gong, Z.; Song, C.; Bai, C.; Zhao, X.; Luo, Z.; Qi, G.; Liu, X.; Wang, C.; Duan, Y.; Yuan, Z., Anchoring high-mass iodine to nanoporous carbon with large-volume micropores and rich pyridine-N sites for high-energy-density and long-life Zn-I₂ aqueous battery. *Sci. China Mater* **2022**, *66* (2), 556-566.
5. Hou, Y.; Kong, F.; Wang, Z.; Ren, M.; Qiao, C.; Liu, W.; Yao, J.; Zhang, C.; Zhao, H., High performance rechargeable aqueous zinc-iodine batteries via a double iodine species fixation strategy with mesoporous carbon and modified separator. *J Colloid Interface Sci* **2023**, *629*, 279-287.
6. Zhang, L.; Zhang, M.; Guo, H.; Tian, Z.; Ge, L.; He, G.; Huang, J.; Wang, J.; Liu, T.; Parkin, I. P.; Lai, F., A Universal Polyiodide Regulation Using Quaternization Engineering toward High Value-Added and Ultra-Stable Zinc-Iodine Batteries. *Adv Sci* **2022**, *9* (13), e2105598.
7. Chen, M.; Zhu, W.; Guo, H.; Tian, Z.; Zhang, L.; Wang, J.; Liu, T.; Lai, F.; Huang, J., Tightly confined iodine in surface-oxidized carbon matrix toward dual-mechanism zinc-iodine batteries. *Energy Stor. Mater* **2023**, *59*, 102760.
8. Du, Y.; Kang, R.; Jin, H.; Zhou, W.; Zhang, W.; Wang, H.; Qin, J.; Wan, J.; Chen, G.; Zhang, J., Lithiation Enhances Electrocatalytic Iodine Conversion and Polyiodide Confinement in Iodine Host for Zinc-Iodine Batteries. *Adv. Funct. Mater.* **2023**, *33* (45), 2304811.
9. Guo, Q.; Wang, H.; Sun, X.; Yang, Y. n.; Chen, N.; Qu, L., In Situ Synthesis of Cathode Materials for Aqueous High-Rate and Durable Zn-I₂ Batteries. *ACS Mater. Lett.* **2022**, *4* (10), 1872-1881.
10. Liu, M.; Chen, Q.; Cao, X.; Tan, D.; Ma, J.; Zhang, J., Physicochemical Confinement Effect Enables High-Performing Zinc-Iodine Batteries. *J. Am. Chem. Soc.* **2022**, *144* (47), 21683-21691.
11. Liu, T.; Wang, H.; Lei, C.; Mao, Y.; Wang, H.; He, X.; Liang, X., Recognition of the catalytic activities of graphitic N for zinc-iodine batteries. *Energy Stor. Mater* **2022**, *53*, 544-551.
12. Liu, W. F.; Liu, P. G.; Lyu, Y. H.; Wen, J.; Hao, R.; Zheng, J. Y.; Liu, K. Y.; Li, Y. J.; Wang, S. Y., Advanced Zn-I₂ Battery with Excellent Cycling Stability and Good Rate Performance by a Multifunctional Iodine Host. *ACS Appl. Mater. Interfaces* **2022**, *14* (7), 8955-8962.